A GENERIC ENERGY FLEXIBILITY EVALUATION FRAMEWORK TO CHARACTERISE THE DEMAND RESPONSE POTENTIAL OF RESIDENTIAL BUILDINGS

Adamantios Bampoulas[1,2], Mohammad Saffari[1,2], Fabiano Pallonetto[1], Eleni Mangina[1,3], and Donal P. Finn[1,2]
[1]Energy Institute, University College Dublin, Dublin, Ireland
[2]School of Mechanical and Materials Engineering, University College Dublin, Dublin, Ireland
[3]School of Computer Science, University College Dublin, Dublin, Ireland

The scope of the current work is to present a fundamental unified framework to quantify and characterise the energy flexibility of electrical and thermal systems commonly found in residential buildings. A quantification framework applicable to multicomponent residential buildings is developed and the energy cost of various demand response actions in the context of locally produced energy is determined. A calibrated white-box model of a residential building using EnergyPlus is utilised towards this end and the associated results are aggregated to formulate daily mappings of energy flexibility. Simulations show that the flexibility potential of each component depends on multiple factors including, inter alia: weather, occupant preferences, energy conversion components, and building thermal characteristics..

INTRODUCTION

The proliferation of distributed electricity generation, particularly from renewable energy resources, and smart metering systems has drawn attention to the role that demand side management can play in improving the operation of the electricity market (COWI, 2016). Demand side flexibility (DSF) or demand-response (DR) has been widely recognised by energy system stakeholders as a key strategy for ensuring the efficiency and sustainability of the electricity system in a cost-efficient way. DR can enhance energy supply security, facilitate greater penetration of renewable energy sources (RES) levels into the grid, and promote market competition and consumer participation. DR allows consumers to strategically change their current consumption patterns by responding to control signals and/or financial incentives. The purpose of these signals is to modify the use of electricity and to optimise the use of networks, as well as the generation and consumption of electricity (CEER, 2014). Demand-side flexibility is referred either as dispatchable flexibility that can be traded on the different energy markets by an aggregator (explicit) or as consumer reaction to price signals (implicit) (SEDC, 2016).

Buildings can be an important source of energy flexibility for the electricity grid, thanks to the increasing use of heat pumps, onsite electricity generation, energy storage, and electric vehicles (Li and Pye, 2018). Although buildings are widely recognised smart grids elements, to date there is no accepted definition of their energy flexibility, mainly due to the different requirements and properties of an energy-flexible building. The high-level definition of an energy-flexible building used as a starting point in this study is as follows (Jensen et al., 2017): "*the ability to manage its demand and generation according to local climate conditions, user needs, and grid requirements. Energy flexibility of buildings will thus allow for demand-side management/load control and thereby demand response based on the requirements of the surrounding grids and the availability of RES, to minimize the CO_2 emissions*".

Background

The different definitions of energy flexibility in buildings are accompanied by numerous and varying flexibility quantification methods. D'hulst et al. (2015) quantify the flexibility of residential electrical appliances by characterising their possible power level changes over a given period; however, the energy costs resulting from these actions are not investigated. Reynders et al. (2017) introduced the concept of storage capacity and storage efficiency in order to investigate the flexibility potential of the thermal mass of a building. Storage capacity refers to the energy that can be added to the thermal mass of a building during a particular DR action, while the storage efficiency is an energy cost indicator associated with that DR action. Nuytten et al. (2013) quantify power and energy flexibility by calculating the associated forced and delayed operation times to analyse the flexibility potential of heat pumps and combined heat and power plants when combined with thermal energy storage. Other works quantify flexibility offered by the building thermal mass either by calculating the amount of energy that can be shifted for a specific duration and the corresponding energy cost (De Coninck and Helsen, 2016) or by introducing a flexibility indicator which assesses

the capability of the building heating system to shift its heating energy from on-peak to off-peak periods (Le Dreau and Heiselberg, 2016). Nevertheless, these studies have mainly focused on the evaluation of the buildings structural thermal mass flexibility or neglect the contribution of onsite energy generation and the cost of individual demand response strategies.

Research Contribution and Scope

In contrast to these works, the methodology presented herein can be applied to various electrical appliances in the residential domain. In addition, it addresses the question of a generalised methodology to calculate the net energy cost of the various DR actions in the context of onsite electricity generation. Specifically, flexibility is assessed in terms of both capacity and associated energy cost by using suitable indicators. The latter can be of interest to various stakeholders of the energy system such as electricity system designers and operators, energy aggregators and building owners. In particular, existing flexibility indicators (i.e., storage capacity and efficiency (Kathirgamanathan et al., 2018), (Bampoulas et al., 2019)) are generalised through the concept of self-consumption during a DR action. These metrics may be interpreted differently by two of the critical stakeholders, namely, building owners and aggregators. Building owners are more interested in using device energy flexibility to minimise their electricity bills albeit without major lifestyle changes. On the other hand, aggregators are more interested in the energy shifting capability of a building in terms of volume, time, and cost, so as to define their bidding strategy. To accurately quantify this capability in case of onsite electricity generation, it is deemed necessary to also account for the onsite energy generated during a DR action. This approach allows not only to calculate the contribution of solar energy to the energy costs of different DR strategies but also to create a unified framework for quantifying the flexibility of both electrical (e.g., electric batteries) and thermal systems (e.g., heat pumps, thermal energy storage).

CHARACTERISATION OF ENERGY FLEXIBILITY

Active DR actions and characteristics

Energy flexibility can be assessed for downward (down-flex) and upward (up-flex) modulations. In a down-flex action, the electrical device power consumption is curtailed and it is restored to normal operation later. Any associated storage medium will thus be recharged allowing it to return to its original state as before the DR action. However, in case of onsite energy generation by renewables during the rebound, the actual energy cost of the DR action is reduced by the pertinent energy amount. Figure 1 depicts a qualitative scenario of a down-flex action when local generation is available – for example, solar power. t_{DR} is the DR event duration, while τ_{RD} and τ_{ID} are the total times of the reduced and increased demand, respectively. The DR event duration and total times of modulated demand are defined differently in the case where the storage medium has slower dynamics. The energy reduction during the DR event is depicted by the area A (green), the fraction of the rebound covered by local generation is depicted by the area C (yellow), the fraction of the rebound covered by the grid is illustrated by the area D (orange), and the whole rebound corresponds to area B (indicated by the black bold line).

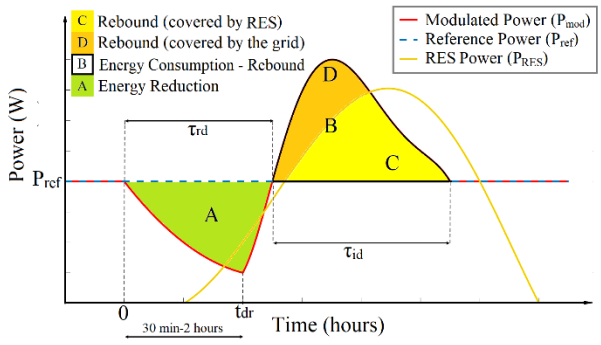

Figure 1 Down-flex action

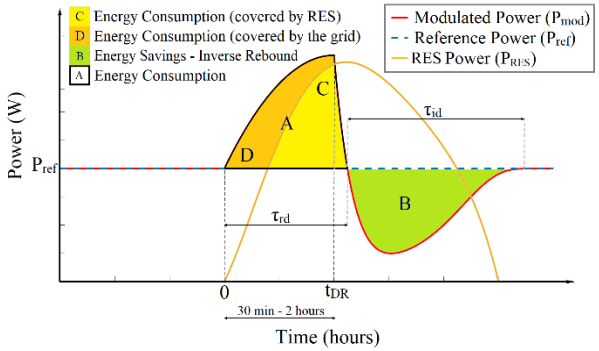

Figure 2 Up-flex action

In an up-flex action, additional energy is consumed by an electrical device and is directly or indirectly stored in an energy storage unit. However, the actual cost of this action is reduced by the coinciding solar energy amount, if it is available. Likewise, in Figure 2, an up-flex action scenario is presented; the energy increase is depicted by the area A (indicated by the black bold line), the grid-covered energy fraction is illustrated by area D (orange), the electricity covered by local generation corresponds to the area C (yellow), and the energy reduction associated to the DR action (inverse rebound) is illustrated by area B (green).

Energy flexibility indicators

- Self-consumption fraction during a DR action

The self-consumption during a DR action (SC_{DR}) is defined as the proportion of increased demand covered by onsite generation. This indicator is a measure of the coincidence between onsite electricity generation and increased demand during a DR action. In down-flex, local electricity generation can sometimes cover the rebound, while in up-flex onsite, electricity generation can under certain conditions cover the energy increase during the DR action. SC_{DR} for both flexibility types is given by equation (1):

$$SC_{DR} = \frac{C}{C+D} = \frac{\int_0^{\infty} (\max(\min(P_{\mathrm{mod}}, P_{res}) - \mathrm{P}_{ref}), 0))dt}{\int_0^{\infty} (P_{\mathrm{mod}} - \mathrm{P}_{ref})^{+} dt} \quad (1)$$

where the "+" and "-" superscripts are $x^{+}=max(x,0)$ and $x^{-}=max(-x,0)$. P_{mod} and P_{ref} stand for the total modulated and reference building load, respectively, while P_{res} is the onsite solar power generation.

- Storage Capacity

The available storage capacity (C_{DR}) of an energy storage unit is defined as the energy amount that can be added or curtailed from the system during an active DR action, subject to the associated boundary conditions. The storage capacity for both flexibility types is given by the area A and is described by equations (2) and (3), respectively:

$$A = C_{DF} = \int_0^{\infty} \left| (P_{\mathrm{mod}} - \mathrm{P}_{ref})^{-} \right| dt \quad (2)$$

$$A = C_{UF} = \int_0^{\infty} \left| (P_{\mathrm{mod}} - \mathrm{P}_{ref})^{+} \right| dt \quad (3)$$

The impact of specific DR events, in terms of net energy purchase, can be only quantified by taking into account the coincidence between the building power change and onsite electricity generation. Thus, the net energy usage from the grid is described by the area D for both Figures 1 and 2 and is calculated by equation (4):

$$D = C_{UF}^{net} = \int_0^{\infty} \max(P_{\mathrm{mod}} - \max(\mathrm{P}_{ref}, P_{res}), 0)dt \quad (4)$$

It is noted that equation (3) resolves from (4), if $P_{RES} = 0$.

- Storage Efficiency

The storage efficiency η_{DF} (equation 5) of a down-flex action is defined as the fraction of the energy cost of an active DR event with respect to the energy reduction achieved during this event:

$$\eta_{DF} = 1 - \frac{D}{A} = 1 - \frac{\int_0^{\infty} \max(P_{\mathrm{mod}} - \max(\mathrm{P}_{ref}, P_{res}), 0)dt}{\int_0^{\infty} \left| (P_{\mathrm{mod}} - \mathrm{P}_{ref})^{-} \right| dt} \quad (5)$$

This indicator takes values between 0 and 1 and depends not only on the relationship between the energy cost and the curtailed energy amount but also on the temporal coincidence between the rebound and onsite generation.

The storage efficiency (η_{UF}) of an up-flex action (equation 6) is defined as the fraction of the energy increase during an active DR event that can be subsequently used to reduce the necessary power to restore the previous control setpoints:

$$\eta_{UF} = \frac{B}{D} = \frac{B}{(1 - SC_{DR})A} = \frac{\int_0^{\infty} \left| (P_{\mathrm{mod}} - P_{ref})^{-} \right| dt}{\int_0^{\infty} \max(P_{\mathrm{mod}} - \max(\mathrm{P}_{ref}, P_{res}))dt} \quad (6)$$

However, this formulation may result in efficiencies greater than 1.0 in the case of increased self-consumption. Thus, equation (6) can be redefined so that efficiencies are within 0 and 1, as per equation (7):

$$\eta_{UF} = \frac{B}{B + (1 - SC_{DR})A} \quad (7)$$

Boundary conditions

- Structural thermal energy storage

The structural TES DR potential is assessed for room thermostat setpoint (ΔT_r) modulations and a duration of t_{dr}. To avoid occupant thermal comfort distortion, the operative temperature changes resulting from the associated DR actions should lie within acceptable limits as per Table 1 (ASHRAE, 2017).

Table 1 Limits on temperature drifts

TIME PERIOD	MAXIMUM ALLOWED OPERATIVE TEMPERATURE CHANGE
30 min	1.1°C (2°F)
1 hour	2.2°C (4°F)
2 hours	2.8°C (5°F)

- Hot water thermal energy storage

The DR potential of a hot water tank system is harnessed by modulating its thermostatic setpoint (ΔT_s) for a duration of t_{dr}. When such a system is coupled with the heating system, DR actions can not only affect the hot water availability, but also the heating system performance. Therefore, to avoid occupant thermal comfort distortion, the acceptable limits of ΔT_s for a given t_{dr} are case-specific and can be only determined by a heuristic analysis.

- Electrical thermal energy storage

Since battery power flows are directly controlled by inverter-based systems, only down-flex actions are considered. Using a battery as a flexibility source comes at an energy cost due to efficiency losses in the inverter and parasitic losses. The rebound in this case is the restoration of the State of Charge (SoC) before the DR action and may occur later depending on the control algorithm. The maximum flexibility potential of a stationary battery is calculated by assuming that it is only used during a DR action, otherwise, it remains inactive at a reference SoC, SoC_{ref}. The associated flexibility potential is harnessed by discharging the battery for a duration of t_{dr}, with a power potential equal to the overall building load, P_b, thereby eliminating electricity purchase from the utility. By considering that $t_{DR} = \tau_{RD}$ (because of the fast dynamics of the battery), equation 2 can be further simplified to equation 8.

$$C_{DF} = \int_0^{\infty} \left| (P_{\mathrm{mod}} - \mathrm{P}_{ref})^{-} \right| dt = \int_0^{\infty} \left| P_b - 0 \right|^{-} = \int_0^{t_{DR}} P_b dt \quad (8)$$

Considering the average discharge and charge efficiencies of η_d and η_c, respectively, the energy amount withdrawn from the battery to cover C_{DF} is C_{DF}/η_d. Also, the battery should absorb C_{DF}/η_d to reach its previous SoC, thus, the power absorbed from the grid is $C_{DF}/(\eta_d \eta_c)$. Consequently, equation (6) can be re-written as shown in equation (9):

$$\eta_{DF} = 1 - (1 - SC_{DR})\frac{B}{A} = 1 - (1 - SC_{DR})\frac{C_{DF}/\eta_d\eta_c}{C_{DF}} = 1 - \frac{1 - SC_{DR}}{\eta_d\eta_c} \quad (9)$$

The coincidence between onsite electricity generation and increased demand can be optimised by suitably controlling their charging power (through an inverter-based system) and the rebound starting time. Therefore, different charging powers and starting times result in different storage efficiencies. For example, if the rebound occurs during a period of zero local energy production, the resulting indicator value is negative and equal to $1-1/\eta_d\eta_c$. Hence, it is important to implement suitable control actions to ensure optimal battery recharging from the local generation. Equation (9) indicates that the lower the battery charging/discharging efficiencies, the greater the necessary self-consumption to ensure a positive storage efficiency for the pertinent DR events.

Energy flexibility mapping

To assess the performance of various DR actions over a winter design day, energy flexibility maps can be developed by imposing consecutive independent DR events. The DR actions, as described earlier, are implemented using 24 independent one hour DR actions with starting times at 0000 hr, 0100 hr, etc. The aggregation of these simulations results in the development of the daily energy flexibility profile. This mapping can be used to give an insight into the performance of the implemented DR actions for the flexibility indicators introduced.

BUILDING DESCRIPTION AND COMPONENTS

This section describes the white-box model used to develop and analyse the DR control algorithms. This model was developed by using EnergyPlus V.9.1 and calibrated by using measured data from the building and an hourly resolution according to ASHRAE guidelines (ASHRAE, 2014). The accuracy of the calibrated building model was evaluated by using the Mean Bias Error (MBE) and the Cumulative Variation Root Mean Squared Error (CVRMSE) as per Mustafaraj et al. (2014); the latter is calculated with respect to the annual error specification based on one year of collected data (2012) (Pallonetto et al., 2016).

Thermal and geometrical properties

As a virtual testbed, a single-storey detached bungalow house located in eastern Ireland is considered. This building type represents approximately 40% of the Irish building stock and is the most common single building category (Pallonetto et al., 2016). A 3D rendering and a picture of the building are illustrated in Figure 3. The dwelling exhibits increased thickness of insulation materials in its opaque elements compared to contemporary standards.

Figure 3 3D rendering and picture of testbed house (Pallonetto et al., 2016)

The house includes twelve rooms and an uninhabited attic space at roof level. The building walls, roof, windows, and floor have U-values of 0.21, 0.21, 1.7, and 0.21 W/m^{2}K (0.037, 0.037, 1.7, 0.037 Btu/h·ft2·°F), respectively.

As a result of its construction (i.e., two-leaf concrete wall with cavity insulation), it exhibits significant passive thermal energy storage capacity. The total surface area of the exterior walls is 187 m^2 (2013 ft^2), excluding associated windows and doors. The slate roof with a surface area of 279 m^2 (3003 ft^2) does not have insulation, while the ceiling is covered with acoustic tiles to ensure both acoustic and thermal insulation. On top of the acoustic tiles, a 200 mm (0.66 ft) layer of fibreglass insulation ensures high thermal resistance due to its low thermal conductivity (0.04 W/mK-0.023 Btu·ft/h·ft^2·°F). The floor area is 208 m^2 (2239 ft^2), and the overall window to wall ratio is 15%, with a 22% and 10% ratio on the south and north facades, respectively.

HVAC system

A ground source heat pump (GSHP) with a rated thermal output of 12 kW constitutes the building space heating system. The GSHP is coupled with a hot water storage tank of 0.8 m^3 (28 ft^3) to provide thermal energy storage. The heating system is depicted in Figure 4. The control setpoints of the GSHP include the room thermostat setpoint T_r and the water tank thermostat setpoint T_{wt}.

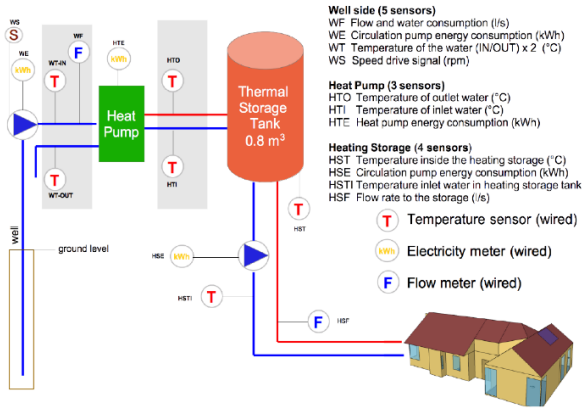

Figure 4 Heat system design and sensor metering (Pallonetto et al. 2016)

Table 2 Thermostatic setpoints

TIME OF THE DAY	TEMPERATURE
00:00-06:00	17 °C (62.6 °F)
06:00-09:00	19 (66.2 °F)
09:00-17:00	16 (60.8 °F)
17:00-00:00	18 (64.4 °F)

The building thermostat setpoints are given in Table 2. It should be noted that the thermostat sensor is located in the hallway, which is a slightly cooler zone within the building, whereas the thermal comfort score is calculated within the living/kitchen area, which is affected by both solar heat gains, as well as internal heat gains of the kitchen.

Stationary Battery

Although the existing house does not incorporate electrical energy storage in this study, a stationary battery with a capacity of 12 kWh is considered in the simulation analysis, with a maximum charging/ discharging power of 8 kW, and a two-way charging efficiency of 85%.

Solar PV plant

The electrical installation includes a PV system with a nominal power of 6 kWp. The PV system is connected to the grid through a single-phase inverter with an efficiency of 95%.

SIMULATION RESULTS

The reference case utilises a winter design day. The minimum and maximum temperatures are -2°C (35.6°F) and 0.4°C (32.7°F), respectively, and the maximum global solar radiation is 368 W/m^2 (34.2 W/ft^2). A heuristic analysis showed that this temperature is the minimum one for which occupant thermal comfort can be achieved during the selected day. Baseline lower and upper water tank temperatures are set to 35°C (95°F) and 55°C (131°F), respectively. Figure 5 illustrates the building power demand excluding the GSHP load, the GSHP power, and solar PV power generation for the day under study. This figure highlights the need to assess the building energy shifting capability and associated energy costs as the solar PV electricity generation is maximised when the heating demand is minimised (due to the reduced room thermostat setpoints during the non-occupancy period).

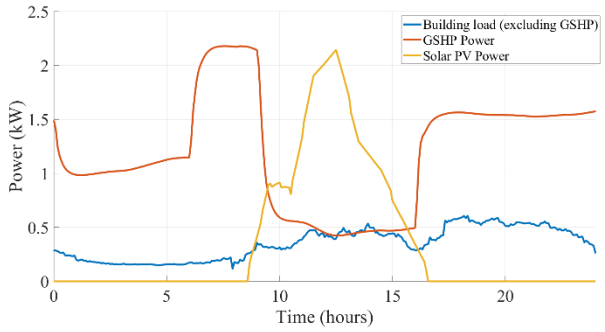

Figure 5 Building power demand excluding the GSHP, GSHP power, and solar PV electricity generation for the winter design day

Downward flexibility analysis

The flexibility potential of the heat pump can be harnessed either by activating the structural TES (passive TES) or the water tank TES (active TES), by modulating T_r and T_{wt}, respectively. The maximum flexibility potential of each control method is evaluated by implementing different control strategies. Notwithstanding that the structural TES maximum flexibility is exploited by considering room thermostatic changes of +/- 2.2°C (4°F) (ASHRAE, 2017), a parametric analysis is carried out to determine the maximum T_{wt} for which occupant thermal comfort is not distorted for hourly DR actions. The results of this analysis have shown that the maximum hourly water tank and room temperature drifts are -6.2 K (11.6°F) and -0.49 K (0.88°F), respectively. As a result, thermal comfort was found not be violated during hourly water tank temperature modulations resulting from its high thermal inertia.

As an example of a down-flex action, an hourly room and a water tank thermostat modulation with a starting time at 0700 hrs is illustrated in Figure 6. It is worth noting that the DR duration and total time of reduced demand are significantly different for room thermostat setpoint modulations due to the slower dynamics of the building envelope. The rebound associated with the room thermostat setpoint modulation exhibits lower magnitudes and higher durations compared to the water tank temperature modulations. This means that rebounds resulting from each modulation can be effectively covered by specific renewables depending on their energy production profile. For example, solar power plants are more suitable to cover rebounds resulting from water tank thermostat modulations due to their limited duration.

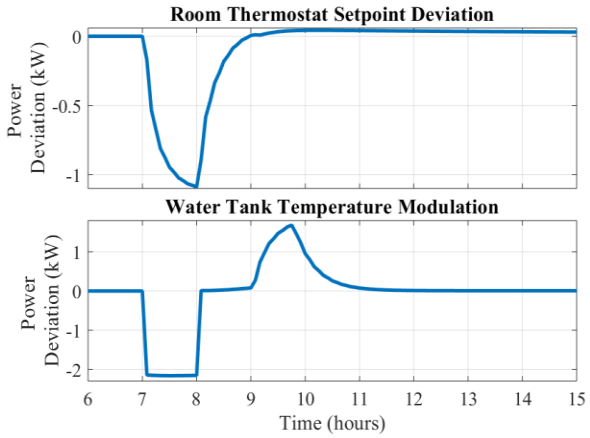

Figure 6 Down-flex DR action between 0700 and 0800 hours for a room thermostat modulation and a water tank temperature modulation

- Energy Flexibility Maps

The storage capacity (Eq. 2) resulting from room and water tank temperature reductions and the stationary battery use is depicted for all 24 independent hourly DR actions in Figure 7. Higher baseline room thermostat setpoints result in higher storage capacities both for room and water tank temperature modulations. This is because the consumption of

the heat pump increases during this period (0600-0900), hence the resulting flexibility margin increases. The battery power depends on the difference between the building power demand and solar power; this results from the discharge of the stationary electric battery to cover the building load. Thus, the storage capacity is zero, when the PV electricity generation exceeds the building demand. Moreover, the higher the room thermostat setpoints, the higher the battery storage capacity due to the increased heat pump consumption.

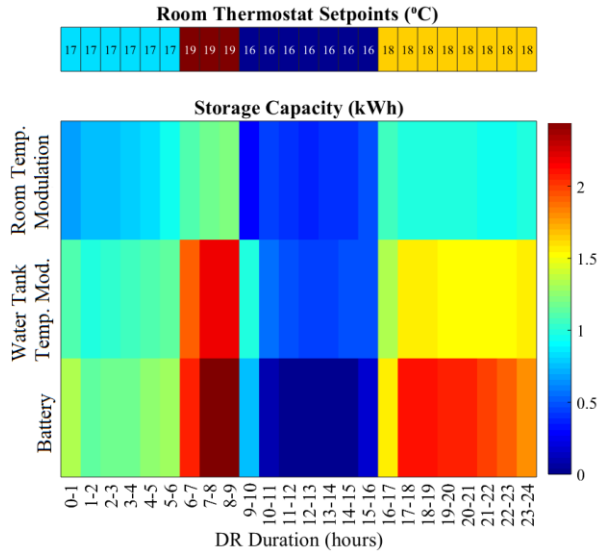

Figure 7 Storage capacity, GSHP (room and water tank temp. modulations) and stationary battery, hourly down-flex DR actions

The self-consumption (Eq. 1) during a DR event and the storage efficiency (Eq. 5) resulting from room and water tank temperature reductions for all hourly DR events are presented in Figure 8. Since the rebounds associated with room thermostat modulations last longer (as depicted in Figure 6), the associated self-consumption is non-zero during this period (0000-1400), even when the PV plant does not produce any power. This happens because the building demand remains greater for up to 10-12 hours after the DR action. In addition, room temperature setpoint modulations exhibit lower self-consumption (up to 40%) because of the long duration of the associated rebounds. When self-consumption is close to zero (1500-0000), the resulting storage efficiency is approximately constant (62%). In fact, the higher the self-consumption, the higher the storage efficiency.

On the other hand, the self-consumption resulting from water tank thermostat modulations follows the same trend as the PV electricity generation (as depicted in Figure 5). This is because the associated rebounds are shorter (as illustrated in Figure 6) and, hence, can be completely covered by onsite generation. The storage efficiency is also maximised during periods of high self-consumption (1000-1400). It is noteworthy that when self-consumption is zero, room thermostat modulations exhibit higher storage efficiency compared to water tank temperature modulations since the latter result in more significant rebounds.

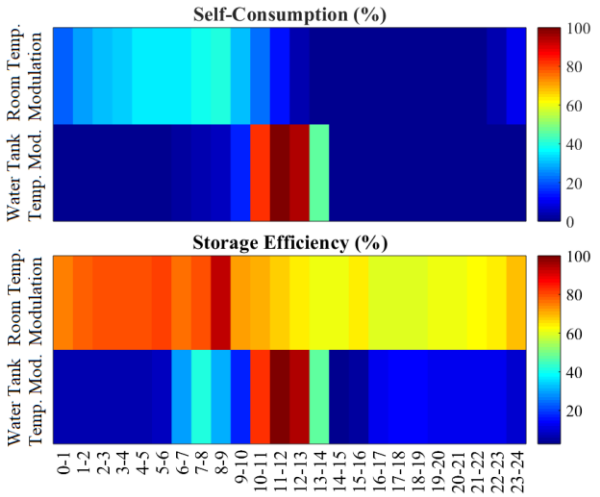

Figure 8 Self-consumption and storage efficiency, GSHP (room and water tank temp. modulations), hourly down-flex DR actions

The energy cost associated with the battery use is calculated by assuming that the rebound duration is one hour. The storage efficiency (Eq. 5) mapping for several rebound starting times are given in Figure 9.

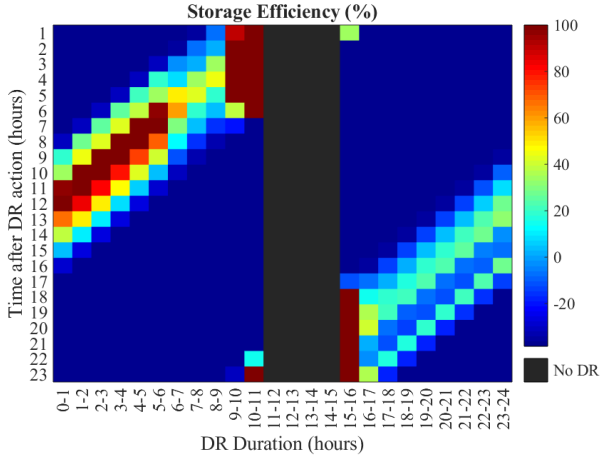

Figure 9 Storage efficiency for the battery, hourly down-flex DR actions, rebounds occurring 1-23 hours after DR actions commencement

The mapping provided in Figure 9 provides the storage efficiency for up to 23 hours after each DR action. The black area corresponds to periods during which no DR actions take place, i.e., periods during which solar PV power exceeds building demand. When solar energy is not available, the storage efficiency is equal to $h_{DF} = 1 - 1/\eta_d \eta_c = -38.4\%$, because self-consumption is equal to zero. When solar energy is available, the efficiency increases and reaches 100% during high electricity generation periods.

Upward flexibility analysis

An upper storage temperature of 55ºC (131ºF) is set for the water tank and it is the minimum baseline water tank temperature for which thermal comfort is maintained. Thus, only downward flexibility actions are considered.

The heat pump up-flex potential is assessed by examining the storage capacity of the room thermostatic modulations, as illustrated in Figure 10. C_{UF} (Eq. 3) is used to assess the GSHP energy shifting capability, while C_{UF}^{net} (Eq. 4) is used to assess the net impact from a grid perspective. The storage capacity during periods of lower baseline room

temperature setpoints is higher due to the lower GSHP consumption. Furthermore, electricity generated by the PV system attenuates the impact of down-flex actions between 1000 and 1600 hrs.

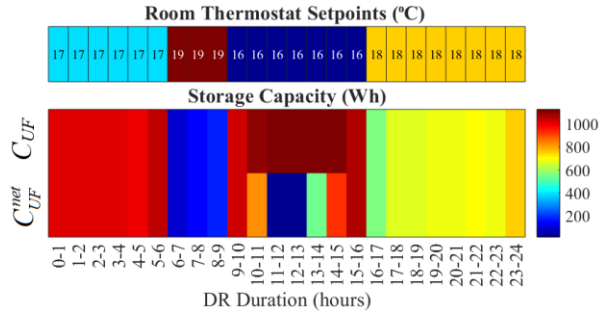

Figure 10 Storage capacity, GSHP (room temp. modulations), hourly up-flex DR actions

Figure 11 illustrates the self-consumption (Eq. 1) during a DR action and the storage efficiency (Eq. 6) for hourly upward modulations of the room thermostat setpoint.

It is observed that room thermostat setpoint modulations can be entirely covered by onsite electricity generation achieving self-consumption and storage efficiency rates equal to 98%. From the above, it can be concluded that onsite solar PV generation is more suitable to cover upward thermostatic modulations for both the room and water tank.

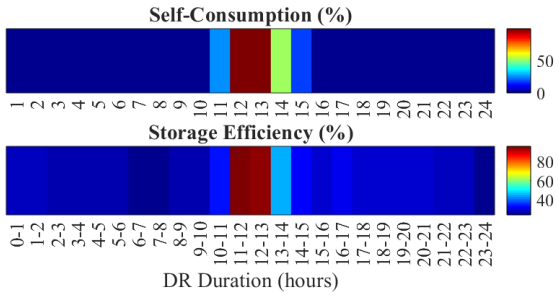

Figure 11 Self-consumption and storage efficiency, GSHP (room temp. modulations), hourly up-flex DR actions

DISCUSSION

The daily flexibility mapping obtained depicts not only the energy shifting capability of different energy storage units but also the corresponding energy costs. These indicators give insights into the energy volumes related to DR actions, as well as the qualitative characteristics of electricity consumption during DR actions. For example, non-zero self-consumption values during periods of zero PV electricity generation are related to prolonged rebounds.

The energy flexibility profiles obtained greatly depend on the selected testbed and associated occupancy profiles. For example, the building thermal characteristics and the heating system type directly influence the power deviation during DR periods and consequently the energy storage capacity and energy cost volumes. This indicates that each building instance energy flexibility can be quantified and characterised by different flexibility maps. This mapping can capture the flexibility potential of individual DR strategies and present it concisely and consistently.

This paper establishes a fundamental methodology applicable to a wide range of electrical and thermal components commonly found in residential buildings. The developed framework is generic and can be applied to all building models which comprise of thermostatically controlled electric heating systems and hot water TES, as well as electrical energy storage, and onsite electricity generation. Nevertheless, the introduced flexibility metrics are subject to boundary conditions which may be dynamic. For example, DR actions associated with hot water TES systems (coupled with domestic hot water and/or heating systems) influence thermal comfort, thus, the pertinent boundary conditions depend on the HVAC system specifications and can be only determined by a heuristic analysis. This means that the proposed methodology should be suitably adjusted to account for the distinct characteristics and configurations of the TES under study.

Occupant preferences impact the thermostatic setpoint selection as well as the non-controllable loads energy consumption. Simulation results show that thermostatic setpoints impact the flexibility margin of individual DR actions and thus the flexibility mapping patterns. An additional occupant related characteristic is the maximum allowed operative temperature change during the activation of the active and passive TES. Even though ASHRAE standards (ASHRAE, 2017) have been adopted in this study, the considered boundary conditions could be more or less strict on the basis of occupant thermal preferences. Furthermore, since the storage efficiency (Eq. 5-6) and self-consumption rates (Eq. 1) depend on the total building load, it is evident that the non-controllable load energy consumption profile influences the net impact of individual DR actions from a grid perspective. Consequently, the flexibility potential of all electrical components is a function of occupancy related attributes, such as thermostat setpoints and use of appliances.

CONCLUSION

In this paper, a generic energy flexibility quantification framework is presented to characterise the flexibility potential of residential buildings both for thermal and electrical systems. Specifically, the flexibility potentials of the building structural thermal mass (passive thermal energy storage), the water tank thermal energy storage (active thermal energy storage), and the stationary battery (electrical energy storage) are evaluated by using the proposed metrics - namely storage capacity, storage efficiency, and self-consumption - during a DR action.

Electricity aggregators can benefit from such flexibility mapping for optimising a portfolio of buildings. Finally, simulations show that the flexibility potential of each component is a characterisitc depending on multiple factors including, inter alia: weather, occupant preferences, energy conversion components, building thermal characteristics, etc.

Future work will also consider electric vehicles as well as more representative days of the heating season. Finally, this methodology will be suitably extended to evaluate the energy flexibility of several residential building instances by using data-driven approaches.

ACKNOWLEDGMENT

This work has emanated from research conducted with the financial support of Science Foundation Ireland under the SFI Strategic Partnership Programme Grant Number SFI/15/SPP/E3125 and additional funding provided by the UCD Energy Institute.

REFERENCES

ASHRAE. (2014). Measurement Of Energy, Demand, And Water Savings ASHRAE Guideline 14-2014.

ASHRAE. (2017). Thermal Environmental Conditions for Human Occupancy, ANSI/ASHRAE Standard 55-2017.

Bampoulas A., M. Saffari, F. Pallonetto, M. de Rosa, E. Mangina, D. P. Finn. (2019). Quantification and characterization of energy flexibility in the residential building sector, 16th IBPSA International Conference and Exhibition, Rome, Italy.

CEER (Council of European Energy Regulators). (2014). CEER Advice on Ensuring Market and Regulatory Arrangements help deliver Demand-Side Flexibility, Brussels, Belgium.

COWI. (2016). Impact Assessment study on downstream flexibility, price flexibility, demand response & smart metering, BRUSSELS: EUROPEAN COMMISSION DG ENERGY.

De Coninck R., L. Helsen. (2016). Quantification of flexibility in buildings by cost curves – Methodology and application, Applied Energy, 162, 653-665.

Demand response flexibility and flexibility potential of residential smart appliances: Experiences from large pilot test in Belgium. (2015), R. D'hulst R., W. Labeeuw, B. Beusen, S. Claessens, G. Deconinck, K. Vanthournout, 155, 79-90.

Jensen S.Ø, A. M. Pomianowska, R. Lollinic, W. Pasut, A. Knotzer, P. Engelmann, A. Stafford, G. Reynders. (2017). IEA EBC Annex 67 Energy Flexible Buildings. Energy and Buildings, 155, 25-34.

Kathirgamanathan A., K. Murphy, M. De Rosa, E. Mangina, D. P Finn. (2018). Aggregation of Energy Flexibility of Commercial Buildings, eSim. Montreal, Canada.

Le Dreeau J., Heiselberg P. (2016). Energy flexibility of residential buildings using short term heat storage in the thermal mass. Energy, 111, 991-1002.

Li P.H., S. Pye. (2018). Assessing the benefits of demand-side flexibility in residential and transport sectors from an integrated energy systems perspective, Applied Energy, 228, 965-979.

Mustafaraj, G., D. Marini, A. Costa, M. Keane. (2014). Model calibration for building energy efficiency simulation. Applied Energy, 130, 72-85.

Nuytten T., B. Claessens, K. Paredis, J. Van Bael, D. Six. (2013). Flexibility of a combined heat and power system with thermal energy storage for district heating, Applied Energy, 104, 583-591.

Pallonetto F., Oxizidis, F. Milano, D. Finn (2016). "The effect of time-of-use tariffs on the demand response flexibility of an all-electric smart-grid-ready dwelling." Energy and Buildings 128, 56-67.

Reynders G., J. Diriken, D. Saelens. (2017). Generic characterization method for energy flexibility: Applied to structural thermal storage in residential buildings, Applied Energy, 198, 192-202.